

Experimental Study of High-Beta Tokamak Stability

M. Machida^(a) and G. A. Navratil
Columbia University, New York, New York 10027
 (Received 10 March 1983)

The stability properties of high-beta tokamak equilibria with $\epsilon\beta_p \geq 1$ and $\langle\beta\rangle$ in the range of 10% have been studied with use of a dual-beam CO₂-laser interferometer system. Two equilibria with $\langle\beta\rangle$ of 9% and 13% were observed to be stable. Another equilibrium with $\langle\beta\rangle$ of 10% was observed to be unstable with the characteristics of a high-toroidal-mode-number ballooning mode.

PACS numbers: 52.35.Py, 52.55.Gb, 52.25.Gj

According to earlier ideal magnetohydrodynamics (MHD) studies^{1,2} tokamak plasma equilibria should be unstable to ballooning modes above moderate beta values of about 3%. Since the fusion power density in a tokamak scales as a strong function of $\langle\beta\rangle$, the volume-averaged beta, these theoretically predicted instabilities could present a serious obstacle to the economic operation of tokamak power reactors. Although several tokamaks (ISX-B,³ PDX,⁴ and Doublet-III⁵) have operated with $\langle\beta\rangle$ in the range of 2.5% to 4.5%, there has been no experimental identification of this instability nor the clear observation of a beta limit for stable operation. Furthermore, recent MHD studies^{6,7} have shown that as beta is increased to the level where the inverse aspect ratio, ϵ , times the average poloidal beta, β_p , is larger than 1, stable tokamak equilibria can again be found. The existence of this "second regime" of stable tokamak operation at a much higher value of beta is therefore a question of considerable importance.

We report in this paper the experimental measurements of the stability properties of the high-beta tokamak equilibria produced in the Torus II tokamak device with $\langle\beta\rangle$ greater than 9%. These equilibria are in the range of parameters where this second regime of stable operation is expected to occur. The Torus II tokamak^{8,9} produces a high-beta equilibrium on a time scale (5 μ sec) faster than the expected MHD instability growth times (10 μ sec). This rapid heating and formation process, employing a fast reversal of the toroidal magnetic field, is described in detail in Ref. 8 and results in the production of an equilibrium which can be studied for about 30 μ sec or about 30 toroidal Alfvén transit times. The measurement of the equilibrium plasma has been reported in Ref. 9 and in Table I we summarize the basic parameters of the machine and the plasma that it produces. All of the results

reported here were obtained with helium plasmas.

The principal diagnostic for the instability studies was a CO₂-laser-scattering/interferometer system. Shown in Fig. 1 is a schematic of the Torus II tokamak and the CO₂-laser diagnostic which uses an 8-W cw laser at 10.6 μ m in the TEM₀₀ mode and 3-mrad beam divergence. We expect from the MHD theory that the toroidal and poloidal wavelengths of unstable modes will be larger than 1 cm for our plasma parameters. Since the scattering angle for such long fluctuation wavelengths is less than the beam divergence, conventional interferometric techniques were used to measure temporal fluctuations in $\int n_e dl$ along various chords through the plasma.

Because of the rapidity with which the equilibrium is formed, we expect any instability to manifest itself as a density fluctuation growing exponentially out of the background noise. We have used a phase-resolved detection technique in order to eliminate possible ambiguities in the interferometer measurements of $\int n_e dl$. These ambiguities could have arisen from refraction of the transmitted beam by the large

TABLE I. Summary of the basic machine and plasma parameters.

Major radius, R	23 cm
Vacuum vessel cross section, $2a$	13 cm
	$2b$ 25 cm
Toroidal field, B_T	3.5 kG
Safety factor at edge, q_a	1.5
Elongation, κ	1.8
Peak beta, β_0	40%
Poloidal beta, β_p	3
Volume-average beta, $\langle\beta\rangle$	(9–13)%
Plasma current, I_p	30 kA
Inverse aspect ratio, ϵ	0.2
Peak temperature, T_e	80 eV
Peak density, n_e	$1.3 \times 10^{15} \text{ cm}^{-3}$

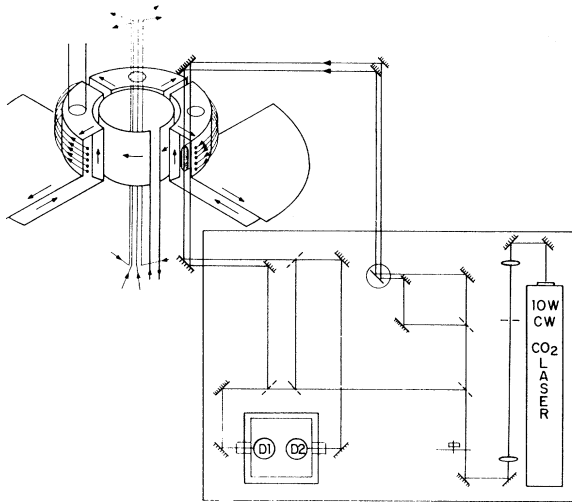


FIG. 1. Schematic diagram of the Torus II tokamak and the CO₂-laser-scattering/interferometer system set up for dual-beam operation with two independent detectors, D1 and D2.

values of $|\nabla n_e|$ present at the edge of the plasma or from a Doppler shift of the transmitted beam induced by radial motion of the entire density profile. The transmitted beam is split into two beams after passing through the plasma and each is heterodyned with a local oscillator onto independent detectors. The path difference between the two beams is adjusted to produce a 90° phase difference between the two detected beat signals. Analysis of the beat signals provides an unambiguous measure of the time-dependent phase variation of the transmitted beam due to fluctuations in $\int n_e dl$ along the path through the plasma. Computer analysis of the phase variation yields $\int n_e dl$ as a function of time as shown in Fig. 2.

The data displayed in Fig. 2 were taken during an equilibrium with a $\langle\beta\rangle$ of about 10% and a growing density fluctuation can be clearly seen beginning about 13 μsec into the tokamak equilibrium phase. It reaches an amplitude of 10% $\delta n/n$ before the plasma is lost, with a growth rate of $2 \times 10^5 \text{ sec}^{-1}$. The oscillation appears to be a single growing mode with a real frequency of 250 kHz and is present with a significant amplitude only on the outer edge (large major radius) of the pressure profile. In Fig. 3 the radial dependence of the density fluctuation is shown. These data were obtained by using two independent transmitted beams to measure $\int n_e dl$ at two radial positions simultaneously, as is shown schematically in Fig. 1. By fixing one beam at

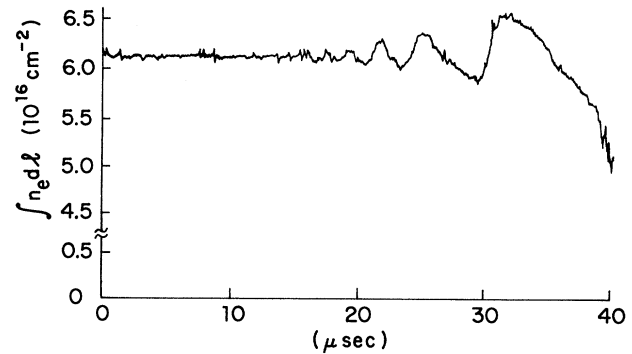


FIG. 2. Observed time history of $\int n_e dl$ during a single unstable discharge with the tokamak equilibrium phase beginning at $t=0$.

the position of maximum instability amplitude and scanning the other radially on a shot-to-shot basis, the relative spatial amplitude distribution of the fluctuation was determined. We observe that the instability amplitude is peaked where $|\nabla p|$ is largest on the outer edge of the profile and is clearly "ballooning" as expected for a ballooning mode in a high-beta tokamak.

The principal diagnostic for the equilibrium pressure profiles was a single-shot, multipoint Thomson scattering system¹⁰ which measures T_e and n_e at ten spatial points along the major radius. Because the electron-ion equilibration time is faster than 2 μsec , we assume $T_i = T_e$ in

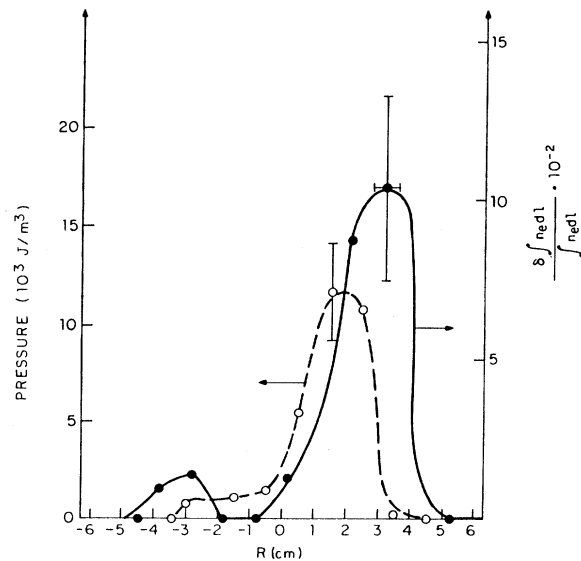


FIG. 3. Pressure profile (open circles) observed at the time of instability onset and the radial distribution of the density fluctuation amplitude (filled circles).

order to compute the local pressure profile at the time of onset of the instability as shown in Fig. 3, as well as the peak and volume-averaged value of beta.

The toroidal wavelength of the mode was measured by using two independent transmitted beams at the same major radius position, but separated in toroidal angle. By measuring the phase shift between these two signals at various toroidal separations the wavelength could be determined. The wavelength was observed to be about 10 cm which would indicate a toroidal mode number of approximately $n = 14 \pm 2$ and a toroidal phase velocity of 2×10^6 cm/sec propagating in the ion diamagnetic drift direction. With use of the relation $m = nq$ for MHD fluctuations, the poloidal mode number, m , would be approximately 16 for these waves. The observed and calculated parameters of this instability are summarized in Table II.

If we compare the observed growth rate with the characteristic growth rates predicted by simple analytic models of resistive tearing,¹¹ ideal⁶ and resistive⁷ ballooning, and collisional drift instabilities¹² for the experimental plasma conditions, we find that the experimental observations are best described by the ballooning-mode growth rates. The calculated growth rate for resistive tearing is less than 10^4 sec⁻¹, which is much slower than the observed value. The observed mode is also not well described by a collisional drift wave because of the locally high beta value, slow predicted growth rate (less than 10^4 sec⁻¹), and propagation in the wrong direction. The ideal and resistive ballooning growth rates, however, were computed to be 7×10^4 and 7×10^5 sec⁻¹, respectively, which bracket the observed value.

We can also compare the measured and computed parameters of this instability with the predictions of a kinetic treatment of ballooning modes.¹³ The frequency and wavelength place this mode in the "intermediate frequency range" which is bounded by ion and electron transit frequencies:

$$\frac{(T_i/m_i)^{1/2}}{qR} < \omega < \frac{(T_e/m_e)^{1/2}}{qR}.$$

For this range, if we assume that trapped-ion and finite-gyroradius effects can be neglected, the toroidal mode numbers would be bounded by $n = 2$ and $n = 16$ with the larger n numbers possessing faster growth rates. These ballooning modes are expected to have a real frequency of approximately ω^* and propagate in the ion diamagnetic

TABLE II. Summary of the observed and calculated parameters of the instability.

Growth rate	$\sim 2 \times 10^5$ sec ⁻¹
Maximum fluctuation amplitude	$\sim 10\%$
Frequency	~ 250 kHz
Toroidal wavelength	10 cm
Toroidal mode number	14
Toroidal phase velocity	2×10^6 cm/sec
Propagation direction	Ion diamagnetic drift direction

drift direction, in good agreement with the experimental observations.

In order to study the effect of a variation in the equilibrium plasma parameters on the observed stability properties, the initial conditions during the plasma formation process were varied, producing different high-beta equilibria. Two such equilibria have been studied in detail and were found to be stable for the duration of the discharge. The first was observed to have a very similar pressure profile to the unstable equilibrium shown in Fig. 3, but with a higher peak beta (45%) and volume-averaged beta (13%). The edge q values were estimated to be the same as those shown in Table I but no experimental data are available on the distribution of q , which is a critical parameter for the determination of the MHD stability of these equilibria. Another equilibrium with a somewhat lower volume-averaged beta value of 9% was produced with a much narrower pressure profile and shorter density-gradient scale length (a maximum $|\nabla p|/p \sim 1$ cm⁻¹ compared with 0.5 cm⁻¹ in the unstable equilibrium). Although finite-Larmor-radius effects may play an important role in the stabilization of this second case, the first does suggest that improved stability has been achieved by increasing the beta value. In all cases the experimental lifetime of the equilibria was unaffected by the presence or absence of instability. Rather, the termination of the discharge was apparently dependent on the decay of the external equilibrium fields and the lifetime is too short in the present device to allow observations of possible nonlinear saturation or disruption of the equilibrium by this instability.

In conclusion, a growing instability has been

observed in tokamak equilibrium in Torus II with $\langle\beta\rangle\sim 10\%$, which is consistent with MHD and kinetic analysis of ballooning modes. Although the experimental observation time is too short to permit the study of the consequences of this instability, the 30- μ sec lifetime is sufficient to observe several growth times, allowing measurements of growth rate, real frequency, propagation direction, and mode number. Perhaps more important than the observation of unstable equilibria at high beta is the observation that equilibria can be created in this very-high-beta regime which appear to be stable for the duration of the experiment. The experiments are too brief to determine that complete stability has been achieved, but they do provide some experimental evidence that more stable and perhaps completely stable tokamak equilibria do exist in this high-beta parameter range.

We wish to thank Dr. D. Oepts for his technical assistance and critical suggestions in the design of the CO₂ scattering system. One of the authors (M. M.) would like to acknowledge fellowship support provided by the Conselho Nacional de Desenvolvimento Científico e Tecnológico-Brazil. This research was supported by U. S. Department of Energy Contract No. DE-AC02-76ET53016.

^(a)Present address: Universidade Estadual de Campinas, Sao Paulo, Brazil.

¹A. M. M. Todd, J. Manikam, M. Okabayashi, M. S. Chance, R. C. Grimm, J. M. Greene, and J. L. Johnson, Nucl. Fusion **19**, 743 (1979).

²B. Coppi, Phys. Rev. Lett. **39**, 939 (1977).

³M. Murakami *et al.*, in *Proceedings of the Ninth International Conference on Plasma Physics and Controlled Nuclear Fusion Research, Baltimore, 1982* (International Atomic Energy Agency, Vienna, 1983).

⁴D. Johnson *et al.*, in Ref. 3.

⁵N. Nagami *et al.*, in Ref. 3; D. Overskei *et al.*, in Ref. 3.

⁶B. Coppi, A. Ferreira, J. W-K. Mark, and J. J. Ramos, Nucl. Fusion **19**, 715 (1979).

⁷H. R. Strauss, W. Park, D. A. Monticello, R. B. White, S. C. Jardin, M. S. Chance, A. M. M. Todd, and A. H. Glasser, Nucl. Fusion **20**, 638 (1980).

⁸G. E. Georgiou, T. C. Marshall, and P. G. Weber, Phys. Fluids **23**, 2085 (1980).

⁹C. K. Chu *et al.*, in Ref. 3.

¹⁰M. Machida, Ph.D. thesis, Columbia University Plasma Physics Laboratory Report No. 89, 1983 (unpublished).

¹¹G. Bateman, *MHD Instabilities* (MIT Press, Cambridge, Mass., 1980), p. 202.

¹²H. W. Hendel and T. K. Chu, *Methods of Experimental Physics* (Academic, New York, 1971), Vol. 9a.

¹³W. M. Tang, J. W. Connor, and R. J. Hastie, Nucl. Fusion **20**, 1439 (1980).